



Cite this: *Toxicol. Res.*, 2018, 7, 191

Mitochondrial toxicity of organic arsenicals: membrane permeability transition pore opening and respiratory dysfunction†

Xiao-Yang Fan,^a Lian Yuan,^a Can Wu,^b Yu-Jiao Liu,^a Feng-Lei Jiang,^b Yan-Jun Hu^c and Yi Liu^{*a,c,d}

In order to clarify the mitochondrial toxicity mechanism of the organic arsenical **MOPIMP** (2-methoxy-4-(((4-(oxoarsanyl) phenyl) imino) methyl) phenol), research was carried out at the sub-cell level based on the previous finding that the compound **MOPIMP** can damage the mitochondria by triggering a burst of ROS. After investigating its influence on isolated mitochondria *in vitro*, it was demonstrated that a high dose of **MOPIMP** with short-term exposure can induce mitochondrial swelling, decrease the membrane potential, enhance the permeability of H⁺ and K⁺, and induce membrane lipid peroxidation, indicating that it can result in an MPT process in a ROS-mediated and Ca²⁺-independent manner. Additionally, MPT was also aggravated as a result of impairment of the membrane integrity and membrane fluidity. In addition, short-term incubation between mitochondria and compound **MOPIMP** promoted the inhibition of respiratory chain complexes I, II, III and IV, as well as damage to the respiration process, which supported the previous finding about the burst of ROS. On the other hand, after long-term exposure by the organic arsenical **MOPIMP**, mitochondrial metabolic dysfunction was triggered, which was in accordance with perturbation of the respiratory chain complexes as well as the respiration process. This work systematically sheds light on the mitochondrial toxicity mechanism of the organic arsenical **MOPIMP**, including induction of the MPT process and inhibition of respiratory metabolism, which provides a potential target for organic arsenicals as anti-tumor drugs.

Received 30th August 2017,
Accepted 22nd November 2017

DOI: 10.1039/c7tx00234c

rsc.li/toxicology-research

Introduction

Arsenicals have shown some complex characterizations.¹ On the one hand, ranked at the top of the US Priority List of Hazardous Substances by the US Environmental Protection Agency (EPA), arsenic as a carcinogen imperiling our safety has been considered a worldwide problem.^{2,3} It has been reported that chronic exposure to arsenic can cause some

cancers, including kidney, bladder, skin and lung cancers, and non-cancerous diseases, such as cardiovascular disease, diabetes, and peripheral vascular disease.^{4–8} Evidence demonstrates that some arsenicals increase their carcinogenicity *via* oxidative stress.^{9,10} On the other hand, some arsenicals, including inorganic arsenicals and organic arsenicals, have shown good anti-tumor activity towards various kinds of cancer cell lines.^{11–14} In particular, arsenic trioxide (ATO) has been successfully used to cure acute promyelocytic leukemia (APL) patients since the 1970s.¹⁵ Regardless of the final effect, there are some similarities in the mechanism of influence, such as an oxidative stress-mediated pathway.^{16,17} Although it is commonly considered that organic arsenicals are less toxic than inorganic arsenicals, they cannot yet be considered benign. More and more evidence demonstrates that organic arsenicals display a higher affinity towards sulfhydryl,¹⁸ better lipophilicity, better stability¹⁹ and higher toxicity^{13,17} than inorganic arsenicals *in vitro*.

A mitochondrion is an important organelle performing pivotal biochemical functions necessary for homeostasis, and it is associated with cell survival as well as cell death.²⁰ Compared with normal mitochondria, a number of additional

^aState Key Laboratory of Virology & Key Laboratory of Analytical Chemistry for Biology and Medicine (MOE), College of Chemistry and Molecular Sciences, Wuhan University, Wuhan 430072, P. R. China. E-mail: yiliuchem@whu.edu.cn; Fax: +8627 68754067; Tel: +8627 68753465

^bState Key Laboratory for the Chemistry and Molecular Engineering of Medicinal Resources, School of Chemistry and Pharmaceutical Sciences, Guangxi Normal University, Guilin 541000, P. R. China

^cCollege of Chemistry and Chemical Engineering, Hubei Normal University, Huangshi 435002, P. R. China

^dKey Laboratory of Coal Conversion and New Carbon Materials of Hubei Province, College of Chemistry and Chemical Engineering, Wuhan University of Science and Technology, Wuhan 430081, P. R. China

†Electronic supplementary information (ESI) available. See DOI: 10.1039/c7tx00234c

metabolic alterations related to mitochondrial function have been observed in cancer cells.²¹ As the main source of ROS generation, mitochondria will inevitably suffer from oxidative damage. Some studies find that arsenic can induce the collapse of mitochondrial membrane potential, a burst of ROS, and mitochondrial membrane permeability transition pore (MPTP) opening *via* binding with adenine nucleotide transporter (ANT), as well as having an impact on ATP production, which means that mitochondria are the major objective for arsenic.^{22–27} Although mitochondrial impairment has been observed, the mechanism varies between different compounds. Moreover, compared with much research on inorganic arsenicals, less attention has been paid to organic arsenicals, let alone research at the sub-cell level.

In the present study, we have found that the organic arsenical **MOPIMP** (2-methoxy-4-(((4-(oxoarsanyl)phenyl)imino)methyl)phenol) (see Scheme S1†) can damage the mitochondria in HL-60 cells by triggering a burst of ROS, but the mechanism of influence is not clear enough.¹⁷ In order to reveal a relatively accurate effect on mitochondria by compound **MOPIMP**, a study on isolated mitochondria is performed. After the systematic study, we found that a high concentration of the organic arsenical **MOPIMP** with short-term incubation can induce mitochondrial swelling, decrease the membrane potential, enhance the permeability of H⁺ and K⁺, and induce membrane lipid peroxidation, which revealed that it can lead to MPT. This observation is similar to the influence on isolated mitochondria by arsenic(III).²⁵ In addition, compound **MOPIMP** was shown to impair the membrane integrity and to increase the membrane fluidity, leading to MPT aggravation. Moreover, inhibition of respiratory chain complexes I, II, III and IV by compound **MOPIMP** triggered respiratory dysfunction. Meanwhile, after long-term exposure to the organic arsenical **MOPIMP**, mitochondrial metabolic dysfunction was triggered by perturbation of the respiratory chain complexes as well as the respiration process, which filled in a research blank about the effect on the respiratory metabolism of isolated liver mitochondria by an organic arsenical. Furthermore, this finding provides a potential target of mitochondrial metabolism for arsenic-based drugs.

Experimental

Materials

Bovine serum albumin (BSA) was purchased from Ruji (Shanghai, China). Rotenone, oligomycin, antimycin A, rhodamine 123 (Rh123), hematoporphyrin (HP), EGTA, cyclosporin A (CsA), ruthenium red (RR), dithiothreitol (DTT), ubiquinol, and carbonyl cyanide 3-chlorophenylhydrazone (CCCP) were purchased from Sigma-Aldrich (St Louis, USA). Cytochrome *c* from bovine heart, β -nicotinamide adenine dinucleotide (NADH), and ndodecyl-h-d-maltoside were obtained from Aladdin (Shanghai, China). 2,3-Dimethoxy-5-methyl-6-decyl-1,4-benzoquinone (DB) was purchased from Biovision (Milpitas, USA). 2,6-Dichlorophenolindophenol (DCPIP) and

reduced cytochrome *c* were obtained from Yuanye (Shanghai, China).

Other common chemicals were of analytical reagent grade and used without further purification. All solutions were prepared with aseptic double-distilled water and samples with arsenicals were handled with care.

Characterization of compound MOPIMP

Partial elemental analyses were performed on a Vario EL III CHNOS elemental analyzer. Infrared spectra were recorded on a Nicolet 380 FT-IR Spectrometer using KBr plates (4000–400 cm⁻¹). NMR spectra were obtained with a Varian Mercury VX300 spectrometer at 300 MHz using TMS as internal reference. MS were recorded on a Bruker Daltonics APE XII 47e and VG707VHF mass spectrometer.

2-Methoxy-4-(((4-(oxoarsanyl)phenyl)imino)methyl)phenol (MOPIMP). Pale yellow and needle-shaped microcrystal. Mp: 102–103.5 °C. Elemental analysis calculated for C₁₄H₁₂AsNO₃: C, 53.02; H, 3.81; As, 23.62; N, 4.42; O, 15.13. Found: C, 52.96; H, 3.78; N, 4.51. IR (KBr): 3316 cm⁻¹ (vs, stretching of O–H); 1621 cm⁻¹ (vs, stretching of CH=N); 1593, 1500, 1423 cm⁻¹ (s, stretching of benzene cycle); 1086 cm⁻¹ (s, stretching of ph-As). ¹H NMR (300 MHz, CH₃OH-d₄): 4.09 (s, 3H); 5.26 (s, 1H); 6.726 (d, 4H); 7.331(m, 3H); 8.401 (s, 1H). ¹³C NMR (100 MHz, CH₃OH-d₄): 58.995(1C), 117.355, 117.760, 119.962, 120.749, 121.768, 122.095 (6C), 130.469, 131.364, 132.586, 133.325, 134.212, 147.326 (6C), 149.333 (1C). ESI-MS, *m/z*: 318 [M + H]⁺.¹⁷

Animals

Female Wistar rats weighing 130–150 g were purchased from the Hubei Center for Disease Control and Prevention (Wuhan, China), and kept in micro-isolator cages with free access to water and food in a temperature-controlled room (22 ± 2 °C). The isolation of rat liver mitochondria was performed in compliance with the Guidelines of the China Animal Welfare Legislation, which has been approved by the Committee on Ethics in the Care and Use of Laboratory Animals of the College of Life Sciences, Wuhan University.

Extraction of mitochondria

A beaker containing fresh liver from Wistar rats was placed in ice water. Subsequently, the liver was minced quickly and washed with solution A three times. The remainder was preserved in a beaker which was chilled in ice water and about 4 g of mince were suspended in 80 mL of solution A with 0.4% BSA added. The suspension was homogenized in a Dounce Tissue Grinder (WHEATON) chilled in ice water. Then the homogenate was centrifuged at 3000g for 2 min. The supernatant was decanted. The supernatant was suspended in solution A and centrifuged at 17 500g for 4 min. Then the resulting deposit was centrifuged at 17 500g for 4 min twice and was in turn suspended in solution A and solution B. Finally, the deposit was preserved in 2.5 mL of solution B'. The Biuret method was utilized to measure the mitochondrial protein

concentration using serum albumin as standard. All the operations above were performed aseptically at 0–4 °C.²⁸

Mitochondrial swelling

Mitochondrial swelling was determined by using an ultra-violet-visible spectrophotometer (UNICO, USA) or a multimode plate reader VICTOR™ X5 (PE, USA) to measure the absorbance at 540 nm for 8 min or 60 min at 25 °C. Mitochondria (0.8 mg protein per mL) were suspended in 2 mL or 200 µL of assay solution and treated with different concentrations (20 µM, 50 µM, 80 µM or 100 µM) of compound **MOPIMP**.^{29,30}

H⁺ and K⁺ permeabilization

The permeabilization of H⁺ or K⁺ to the mitochondrial inner membrane was detected in 2 mL of assay solution treated with **MOPIMP** (20 µM, 50 µM, 80 µM or 100 µM). Valinomycin was added into the assay solution to ensure that K⁺ had passed completely through the mitochondrial inner membrane. Mitochondrial permeabilization was tested by using an ultra-violet-visible spectrophotometer (UNICO, USA) to measure the absorbance at 540 nm for 8 min at 25 °C.³¹

Anisotropy

The change in fluorescence excitation anisotropy (*r*) of hematoporphyrin (HP) bonded to the mitochondria was used to evaluate the fluidity of the mitochondrial membranes.³² The anisotropy value was obtained by suspending mitochondria with added HP in 2 mL of assay solution (0.2 M sucrose, 10 mM Tris, 10 mM Mops, 1 mM Na₃PO₄·10H₂O, 10 µM EGTA, 3 µg mL⁻¹ oligomycin, 5 mM succinate, supplemented with 2 µM rotenone, pH 7.3) and treating them with **MOPIMP** (20 µM, 50 µM or 100 µM). The assay was performed at 25 °C and under magnetic stirring by using an LS 55 fluorescence spectrophotometer (PE, USA) ($\lambda_{\text{ex}} = 520 \text{ nm}$, $\lambda_{\text{em}} = 626 \text{ nm}$).

Respiration

Mitochondria (1 mg of protein) were added into 1 mL of mitochondrial buffer solution (100 mM sucrose, 10 mM Tris, 10 mM Mops, 2 mM MgCl₂, 50 mM KCl, 10 mM K₂HPO₄, 1 mM EDTA, 5 mM succinate and 2 µM rotenone). State 4 was initiated by the addition of 1 M succinate alone, state 3 was initiated by adding 1 M succinate and 250 µM ADP into the mitochondrial buffer solution, and uncoupled respiration was initiated by the addition of 3 mM DNP. The level of oxygen was detected and recorded by a computer connected to a Clark Oxygen Electrode (Hansatech Instruments, Norfolk, UK). All the operations above were performed at 25 °C and under magnetic stirring.

Microcalorimetry

There was 1 mL of buffer in all in an ampoule containing solution B', 5 mg of protein per mL of mitochondria, 15 mM pyruvate, and various concentrations (5 µM, 10 µM, 15 µM or 20 µM) of compound **MOPIMP**. These operations were performed at 4 °C. Then the samples were put into a TAM III (TAM III, TA Instruments, New Castle, USA) instrument and

the temperature was set at 30 °C. When the complete thermogenic curves were shown on screen, data collection was terminated.^{33,34}

Evaluation of respiratory chain complex I, II, III and IV activities

All assays were carried out in 200 µL final volume with 4–5 µg of mitochondrial proteins. The absorbance was monitored by a multimode microplate reader (Tecan Spark® 10 M, Switzerland) for at least 3 min. Mitochondria were incubated with **MOPIMP** (2.5 µM, 5 µM or 25 µM) in a specific buffer for 3–5 min before the initiation.

CI: mitochondria were incubated with drugs in 10 mM Tris-HCl buffer (pH 8.0) for 3 min. After incubation with a reaction buffer containing 80 µM 2,3-dimethoxy-5-methyl-6-decyl-1,4-benzoquinone (DB), 1 mg mL⁻¹ of BSA, 3 mM NaN₃, and 0.4 µM antimycin for another 5 min, oxidation of NADH (200 µM) was monitored at 340 nm.

CII: after the mitochondria were suspended in 50 mM potassium phosphate buffer pH 7.4, a reaction buffer consisting of 10 mM succinate, 50 µM 2,6-dichlorophenolindophenol (DCPIP), 3 mM NaN₃, 2 µM rotenone and 2 µM antimycin was added, followed by the addition of 20 µM DB as the initiation reagent. The reduction of DCPIP in association with CII-catalyzed DB reduction was measured at 600 nm.

CIII: mitochondria were incubated in 50 mM Tris-HCl buffer, pH 7.4 containing 1 mM EDTA, 250 mM sucrose, 3 mM NaN₃, and 30 µM oxidized cytochrome *c*. Then 80 µM ubiquinol was added and the reduction of cytochrome *c* was measured at 550 nm.

CIV: mitochondria were suspended in 10 mM Tris-HCl pH 7.0 consisting of 25 mM sucrose, 120 mM KCl, and 0.025% ndodecyl-h-d-maltoside. After addition of 50 µM reduced cytochrome *c*, the oxidation of cytochrome *c* was measured at 550 nm.

The samples including specific inhibitors, namely CI (rotenone, 5 µM), CII (sodium malonate, 10 mM), CIII (antimycin, 4 µM), and CIV (NaN₃, 3 mM), were tested to determine the specificity of the respiratory complexes activities.

Transmission electron microscopy of mitochondria

Mitochondria with various concentrations (20 µM, 50 µM or 100 µM) of **MOPIMP** were handled based on the literature.³⁵ The ultrastructure of mitochondria was observed with a transmission electron microscope Tecnai G20 Twin (FEI, Hillsboro, USA).

Mitochondrial membrane potential ($\Delta\Psi_m$)

The change in mitochondrial membrane potential was monitored by observing the change in fluorescence emission intensity of 250 µM Rh123.^{36,37}

Measurement of lipid peroxidation

Mitochondrial membrane lipid peroxidation was assessed by the consumption of oxygen using a Clark Oxygen Electrode. Mitochondria with compound **MOPIMP** (20 µM, 50 µM, 80 µM

or 100 μM) were injected into a stirred lipid peroxidation medium (1 mL) consisting of 175 mM KCl, 10 mM Tris-HCl, and 3 μM rotenone, pH 7.4. Membrane lipid peroxidation was initiated by the addition of 1 mM ADP/0.1 mM Fe^{2+} . The iron(II) solution must be prepared before using.

Determination of cytochrome *c*

500 μL of mitochondria and different concentrations of **MOPIMP** (20 μM , 50 μM , 80 μM or 100 μM) were suspended into 1.5 mL of buffer solution. The content of cytochrome *c* was determined by a Rat Cyt-*C* Kit and a microplate reader (ELX800, BioTek, USA).

Results and discussion

Organic arsenical MOPIMP induced the opening of mitochondrial permeability transition pore (MPTP)

The mitochondrial membrane is sensitive to exposure to arsenicals. As shown in Fig. 1, there was no change in the absorbance at 540 nm, indicating that the solvent made no difference to the mitochondria. However, when the mitochondria were incubated with compound **MOPIMP**, the decrease in absorbance at 540 nm demonstrated that mitochondrial swelling took place.³⁸ Furthermore, the swelling tendency was proportional to the testing concentration of **MOPIMP**. Mitochondrial swelling occurs as a result of an increase in mitochondrial matrix concentration.³⁹ Swelling is a symptom of mitochondrial dysfunction, and simultaneously it is one of the most important signals for the opening of MPTP.⁴⁰

As another typical marker for mitochondrial permeability transition pore opening,⁴¹ the mitochondrial membrane potential in isolated mitochondria was assessed through an evaluation of Rh123 fluorescence intensity with or without **MOPIMP**. The fluorescent probe Rh123 could enter into the mitochondria due to the membrane potential ($\Delta\Psi_{\text{m}}$). When $\Delta\Psi_{\text{m}}$ collapses, Rh123 is released into the matrix and then the fluorescence intensity increases. Here we can see from Fig. S1† that compound **MOPIMP** destroyed the mitochondrial membrane potential and the amplitude of fluorescence reduction

was synchronous with the increasing concentration of **MOPIMP**.

The proton gradient between both sides of the mitochondrial inner membrane forms the membrane potential ($\Delta\Psi_{\text{m}}$). The variation in mitochondrial membrane permeability is associated with the formation of a proton gradient. Under normal circumstances, the mitochondrial inner membrane intrinsically has a low permeability to charged species and there is a mitochondrial membrane potential. In addition, there are inner membrane channels which mediate cation uptake across the inner membrane and the conductance is tightly controlled.⁴¹ Mitochondria maintain an H^+ gradient depending on the entry and efflux of H^+ . H^+ is available *via* the electron transfer chain and the K^+ - H^+ exchange channel. Simultaneously, it is discharged by means of ATP synthesis and proton leak. K^+ channels contribute to maintaining K^+ homeostasis in the cell and take an important role in apoptosis. K^+ influx depends on K^+ channels and K^+ extrusion is through the K^+ - H^+ exchange. The effects on membrane permeability to H^+ and K^+ were investigated further. The decrease in absorbance at 540 nm showed that **MOPIMP** enhanced the membrane permeability to both H^+ and K^+ (Fig. 2). When the mitochondrial inner membrane is destroyed by the organic arsenical **MOPIMP**, K^+ will be available to the mitochondrial matrix. An excess of K^+ can not only break the balance of K^+ and H^+ , but can also increase the concentration of the mitochondrial matrix and then cause mitochondrial swelling as a result of water influx. If H^+ in the mitochondria is in a state of imbalance, it may cause depolarization of the mitochondrial membrane and the collapse of the inner membrane potential ($\Delta\Psi_{\text{m}}$).

Much research has shown that mitochondrial membrane permeability transition (MPT) plays an important role in mitochondrial dysfunction, as well as in a variety of toxic, hypoxic, and oxidative forms of cell injury and apoptosis.^{42,43} As the outer membrane is ruptured and the inner membrane is damaged because of swelling, a series of pro-apoptosis proteins, including cytochrome *c*, pro-caspases, and AIF, could be released into the cytoplasm.⁴⁴ Furthermore, these factors activate downstream signals and ultimately lead to apoptosis. In our study, the level of cytochrome *c* was determined by the Rat

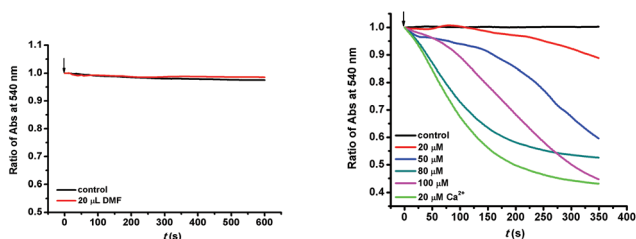


Fig. 1 Induction of isolated mitochondrial swelling in the presence of compound **MOPIMP**. The solvent (20 μL DMF) made a negligible difference to mitochondrial swelling and 20 μM Ca^{2+} was used as the positive sample to examine the effect on swelling. The experiment was repeated thrice.

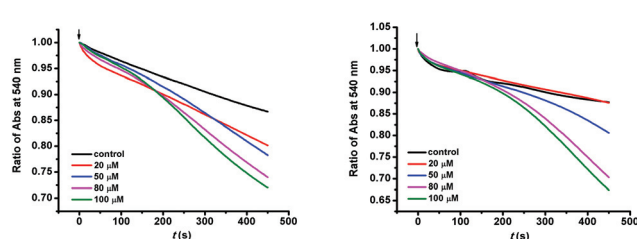


Fig. 2 Permeabilization of the mitochondrial inner membrane. Compound **MOPIMP** increased the permeability of H^+ (left) and K^+ (right) to the mitochondrial inner membrane, showing up as a decline in absorbance at 540 nm in a concentration-dependent way. The experiment was repeated thrice.

Cyt-C Kit. With the addition of compound **MOPIMP**, the release of cytochrome *c* increased (Fig. S2[†]). From these experimental results, which confirmed each other, it was concluded that the organic arsenical **MOPIMP** can induce the MPT process.

The mechanism triggering MPT by the organic arsenical **MOPIMP**

In order to explore the mechanism of MPT induction, several protective reagents were introduced in the research.

CsA can interact mainly with cyclophilin D (Cyp-D), which resides in the mitochondrial matrix, but associates with the inner mitochondrial membrane during MPT, thus inhibiting the opening of the mitochondrial permeability transition pore.⁴⁵ On the base of the enzymatic activity of Cyp-D, it is linked tightly to the conformational change in an inner membrane channel such as ANT, as a result of an increase in inner membrane permeability.⁴⁶ We found that a relatively small amount of CsA (10 μM) can protect the mitochondria from swelling entirely (Fig. 3a), which was evidence to support the opening of the mitochondrial permeability transition pore.

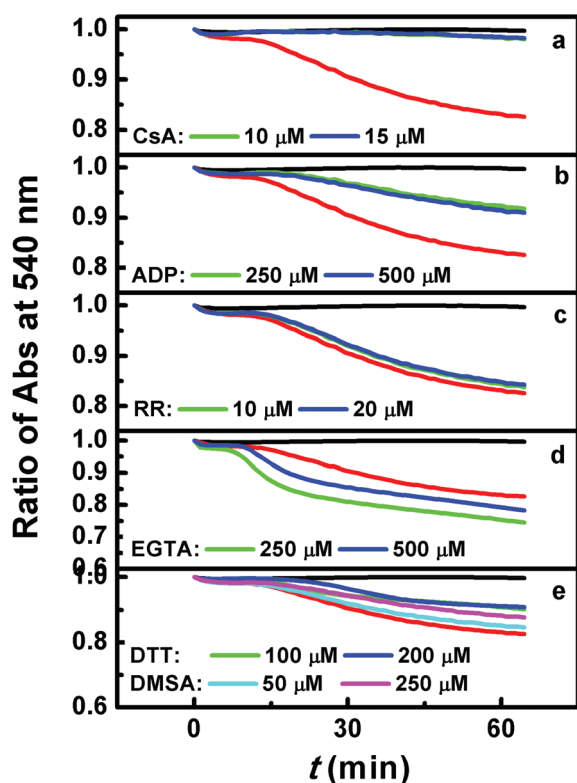


Fig. 3 MPT mechanism induced by compound **MOPIMP**. Mitochondrial swelling was negligible in the absence of **MOPIMP** (black line) and was apparent in the presence of 20 μM compound **MOPIMP** (red line). (a) After treatment with CsA, mitochondrial swelling in the presence of 20 μM compound **MOPIMP** was inhibited entirely. (b) The addition of ADP in advance can help prevent swelling to some degree. Neither RR (c) nor EGTA (d) deterred the swelling induced by compound **MOPIMP**. In contrast, treatment with DTT or DMSA (e) showed a partial protective effect on mitochondrial swelling. The experiment was repeated thrice.

However, neither the specific inhibitor RR for mitochondrial Ca^{2+} transport nor the specific calcium chelator EGTA can suppress the mitochondrial swelling caused by compound **MOPIMP** (Fig. 3c and d). This evidence supported the proposal that the organic arsenical **MOPIMP** induced MPT opening in a calcium-independent manner.

DTT is a kind of strong reducing agent. It can restore disulfide bonds and prevent the formation of disulfide bonds. Reports suggest that agents that act as scavengers of ROS, such as DTT, can inhibit Ar_2O_3 -induced apoptosis as well as the organic arsenicals-mediated apoptosis.^{17,47} Furthermore, some dithiols in small molecules, such as DMSA and DTT, or in macro-molecules like pyruvate dehydrogenase (PDH) and thioredoxin (Trx) show high affinity for arsenic, which is a possible mechanism for detoxication or toxication of arsenicals.^{18,48} As shown in Fig. 3e, 100 μM DTT can also block mitochondrial swelling to some degree, similar to DMSA. These observations demonstrated that the burst of ROS or the conformational change of some vital proteins by the disturbance of residues containing thiols *via* an interaction between arsenic and sulfhydryl may be closely related to MPT.

Although it is in doubt as a central PTP component, adenine nucleotide translocase (ANT) is still associated with the modulation of MPT. There are two distinct conformational states for ANT based on the cytosolic ("c") or matrix ("m") location of the nucleotide binding site, which can be stabilized by atractyloside/carboxyatractyloside or ADP, leading to the stimulation or inhibition of MPT, respectively.⁴⁹ It is found that ANT is one of the targets of arsenites within MPTP, including some inorganic or organic arsenicals.^{24,26} As revealed in Fig. 3b, mitochondrial swelling was reduced after treatment with 250 μM ADP, which indicated that the organic arsenical **MOPIMP** may perturb the ANT conformation *via* reacting with the sulfhydryl therein to open the mitochondrial permeability transition pore.

Based on the experimental results, it was concluded that exposure to a higher concentration of the organic arsenical **MOPIMP** can induce the opening of the mitochondrial permeability transition pore, leading to mitochondrial swelling, collapse of the mitochondrial potential and enhanced membrane permeability by interference with the ANT conformation in a ROS-mediated and Ca^{2+} -independent manner even during the short term.

The mitochondrial membrane damage induced by compound **MOPIMP**

Transmission Electron Microscopy is an intuitive means to confirm that the organic arsenical **MOPIMP** damages mitochondria. The influence on mitochondria with exposure to **MOPIMP** is shown in Fig. 4. Mitochondria extracted from rat liver maintained the integrity of the classical ultrastructure, containing a well-defined outer membrane, a narrow inter-membrane space, and compact cristae. However, with the addition of compound **MOPIMP**, the electron density in the mitochondria declined, mitochondrial membrane underwent swelling, and the shape became irregular or the membrane

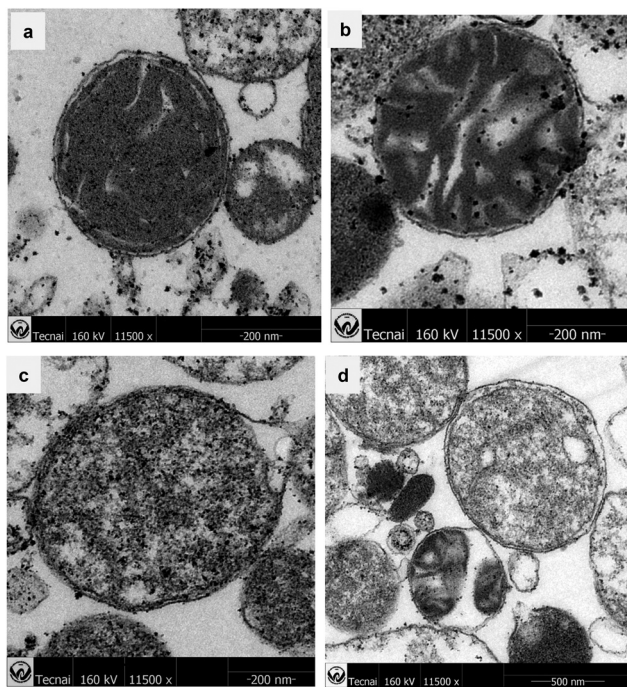


Fig. 4 Ultrastructure of mitochondria treated with different concentrations of **MOPIMP**. (a) The isolated mitochondria without compound **MOPIMP** maintained an intact structure and higher electron density. Compound **MOPIMP** was added in different concentrations: 20 μM (b), 50 μM (c), 100 μM (d). With the addition of compound **MOPIMP**, the mitochondrial electron density declined in a dose-dependent manner. The damage also included the irregular shape (b), mitochondrial swelling (d) and even a ruptured membrane (c).

even ruptured. This was in accordance with the result that the organic arsenical **MOPIMP** impaired the mitochondrial membrane, aggravating the MPT process.

Additionally, mitochondrial membrane fluidity is another marker characterising the mitochondrial membrane function. Since HP will mainly enrich the polar region and protein regions of the phospholipid bilayer on the inner mitochondrial membrane, it can cause the anisotropic value r to rise.⁵⁰ Once the mitochondrial membrane was damaged, HP could be released into the solution, leading to the anisotropic value r declining and the membrane fluidity increasing. The increase in membrane fluidity reflects a conformational change of the pore-forming protein or proteins and it then potentiates the intrinsic proton permeability of the lipid bilayer, the so-called proton leak.⁵¹ In Fig. S3,† we can see that the anisotropic value declined and the membrane fluidity increased when the mitochondria were treated with compound **MOPIMP**, which demonstrated that compound **MOPIMP** may disturb some mitochondrial proteins located in the polarity protein region on the inner mitochondrial membrane. Meanwhile, it has been proved to give rise to proton leak, which is in accordance with the depolarization and permeabilization of mitochondria induced by **MOPIMP**. Thus, a high concentration of compound **MOPIMP** can damage the mitochondrial membrane even for a short contact.

The influence of mitochondrial respiration and impairment of respiratory chain complex activities in the presence of **MOPIMP**

As the “energy factory” in cells, mitochondria’s main function is to provide energy. Thus, it is necessary to detect the influence on mitochondrial respiration by the organic arsenical **MOPIMP**. Utilizing a Clark Oxygen Electrode, the change in mitochondrial respiration was monitored. In the absence of compound **MOPIMP**, both the high respiratory rate of state 3, characterizing the function of the respiratory chain as well as ATP synthesis, and the relatively low respiratory rate of state 4, characterizing the mitochondrial inner membrane, revealed that the mitochondria *in vitro* were intact (see Fig. 5). In the presence of **MOPIMP**, respiration in state 3 showed a significant decrease, which demonstrated that compound **MOPIMP** can inhibit the function of the mitochondrial respiratory chain. However, respiration in state 4 and the DNP-uncoupled state were stimulated by a low concentration of compound **MOPIMP** while they were inhibited by a high level of exposure, which is a feature of a typical uncoupling agent, as a result of the collapse of the membrane potential induced by a proton leak.⁵² This result is in accord with the increase in membrane fluidity, as well as the depolarization and permeabilization of the mitochondria. The respiratory control ratio (RCR = respiration rate of state 3/respiration rate of state 4) decreased with the addition of compound **MOPIMP**, which indicated a certain amount of damage to the mitochondrial respiratory function.

To further explore the toxicity of organic arsenicals on the respiratory chain, assessments of the activities of mitochondrial respiratory chain enzyme complexes, including complexes I, II, III and IV, were performed one by one. As shown in

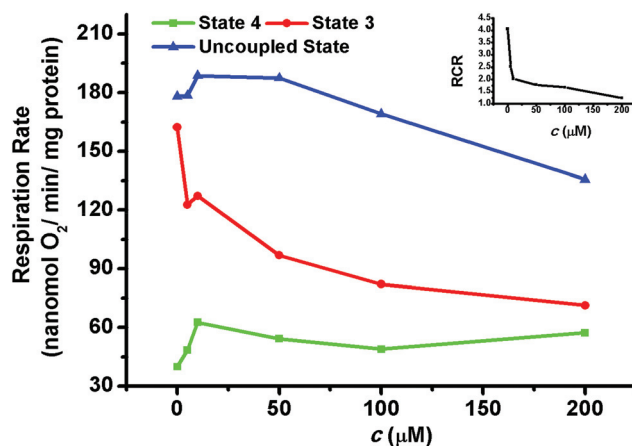


Fig. 5 The effect of mitochondrial respiration in the presence of compound **MOPIMP**. Compound **MOPIMP** was added in different concentrations: 0 μM , 5 μM , 10 μM , 50 μM , 100 μM , 200 μM . With the addition of compound **MOPIMP**, respiration in state 3 (red line) decreased. Respiration in state 4 (green line) and the DNP-uncoupled state (blue line) were stimulated by a low concentration while they were inhibited by a high level of exposure. The respiratory control ratio (RCR = respiration rate of state 3/respiration rate of state 4, black line) also decreased after the addition of **MOPIMP**. The experiment was repeated thrice.

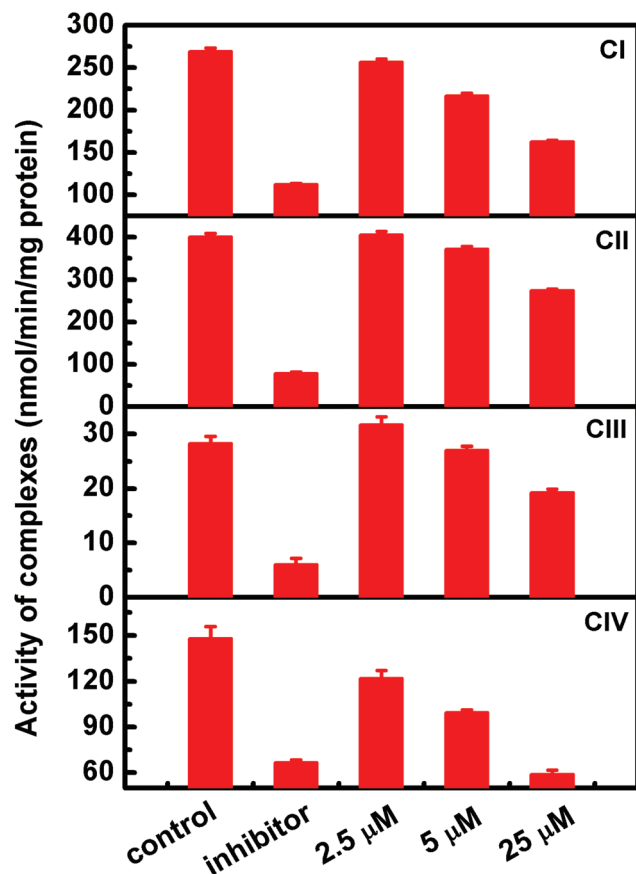


Fig. 6 The effect on activities of respiratory chain complexes I, II, III and IV by the organic arsenical **MOPIMP**. The specific inhibitors added to the four complexes are 5 μM rotenone (CI), 10 mM sodium malonate (CII), 4 μM antimycin (CIII), and 3 mM NaN_3 (CIV), respectively. After incubation with compound **MOPIMP** for 3–5 minutes, the absorbance at a specific wavelength was monitored for at least 3 minutes. The experiment was repeated twice.

Fig. 6, the addition of compound **MOPIMP** influenced the activities of mitochondrial respiratory chain enzyme complexes. Exposure to a high concentration of compound **MOPIMP** (25 μM) can obviously suppress the activities of the four complexes. A low concentration of compound **MOPIMP** (5 μM) had almost no impact on complex II. What is more, the activities of complex I and III showed a drop of 15% to 20%. However, there was a significant destruction of complex IV when it was treated with 5 μM **MOPIMP**. As the terminal enzyme complex of the electron transport chain, complex IV (cytochrome *c* oxidase) is where over 90% of the oxygen is consumed, which largely controls mitochondrial respiration.⁵³ Because compound **MOPIMP** induced a decrease in the activity of complex IV, there was no doubt that mitochondrial respiration was interfered with, which was proved by the observation that a higher concentration of compound **MOPIMP** inhibited oxygen consumption and induced a decrease in the mitochondrial respiratory control ratio (RCR). Reports have pointed out that complexes I and III are often linked to the generation of ROS.⁵⁴ The ROS-mediated MPT process by compound

MOPIMP was consistent with the inhibition of complexes I and III. Accumulation of a high level of ROS may make some oxidative modifications involving reactive cysteine residues located in the complexes and some phospholipids essential for respiratory chain complexes.^{55,56} Furthermore, we found that compound **MOPIMP** indeed triggered the induction of lipid peroxidation due to the generation of ROS in isolated mitochondria (Fig. S4†). These findings demonstrated that ROS were produced through dependent perturbation of the respiratory chain complexes by compound **MOPIMP**, but were also connected with their inhibition. Thus, it was suggested that the respiratory chain complexes I, II, III and IV inhibited by organic arsenical **MOPIMP** were linked to enhanced ROS production, resulting in respiration dysfunction.

The influence of the organic arsenical **MOPIMP** on mitochondrial metabolic thermogenesis

The mitochondrial respiratory chain is associated with ATP production, as well as metabolic thermogenesis. Considering the organic arsenical **MOPIMP**-mediated interference with mitochondrial respiratory chain complexes and the respiration process, we assessed mitochondrial metabolic thermogenesis in the presence of compound **MOPIMP**. As revealed in Fig. 7, the thermogenic curve of control isolated mitochondria contains four phases: lag phase, activity recovery phase, stationary increase phase and decline phase. The lag phase often takes about 10 hours to adapt to the physiological environment. Mitochondria undergo a stationary phase lasting approximately 25 hours after a short activity recovery phase of from

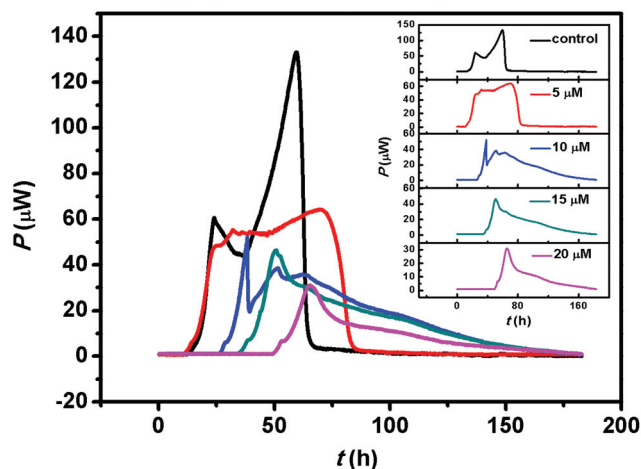


Fig. 7 The thermogenic curves of isolated mitochondria with pyruvate as substrate. There are four phases in the thermogenic curve of control isolated mitochondria (black line): lag phase, activity recovery phase, stationary increase phase and decline phase. After incubation with various concentrations of organic arsenical **MOPIMP** for a long period, the heat output curves were obtained and analyzed for acquisition of thermogenic parameters. The addition of **MOPIMP** induced an extension of the lag phase, a delay in the activity recovery phase, a decrease in the rate constant, a decline in the maximum power output and a drop in the total heat output. The stationary increase phase even disappeared upon exposure to a high dose. The experiment was repeated thrice.

10 h to 25 h. Owing to the oxygen and nutrition being exhausted, there is an obvious decline phase in the last part of the heat generation curve. However, incubation with the organic arsenical **MOPIMP** drastically inhibited the metabolic thermogenesis and triggered the mitochondrial metabolic dysfunction in a concentration-dependent manner.

Based on the thermokinetic equation below, the metabolic parameters can be obtained:^{34,57}

$$\ln P_t = \ln P_0 + kt \quad (1)$$

where P_t and P_0 are the heat output power at a specific time and the initial time, respectively; k represents the rate constant of the lag phase. All the above parameters and other parameters, such as total heat output (Q), maximum power output (P_m), and the maximum power output time (t_m), are displayed in Table S1.† Even though compound **MOPIMP** at a lower concentration (10 μM) also can induce the extension of the lag phase, a delay in the activity recovery phase, a decrease in the rate constant (k), a decline in the maximum power output (P_m) and a drop in total heat output (Q). Furthermore, the stationary increase phase even disappeared when exposed to a higher level of **MOPIMP** for long-term incubation. The inhibition of mitochondrial thermogenesis as a result of inhibition of the respiratory process was linked to the mitochondrial dysfunction. So it was concluded that interference with respiratory chain complexes as well as the respiration process by the organic arsenical **MOPIMP** triggered the mitochondrial metabolic dysfunction after long-term or high-concentration exposure.

Conclusion

The findings in our research could help shed light on the organic arsenicals' mitochondrial toxicity. Based on the observations above, it can be summarized that a high concentration of the organic arsenical **MOPIMP** can induce the mitochondrial swelling prevented by CsA, ADP, DTT and DMSA, decrease the membrane potential, enhance the permeability of H^+ and K^+ , induce membrane lipid peroxidation, impair respiration, inhibit respiratory chain complexes I, II, III and IV, damage the membrane integrity, increase the membrane fluidity, and trigger cytochrome *c* release, which demonstrate that it can lead to MPT in a ROS-mediated and Ca^{2+} -independent manner even with short-term exposure. Meanwhile, after long-term exposure to organic arsenical **MOPIMP**, perturbation to the respiratory chain complexes as well as to the respiration process can trigger mitochondrial metabolic dysfunction. These data will help us understand the toxicity of organic arsenicals better.

Conflicts of interest

There are no conflicts of interest to declare.

Acknowledgements

We gratefully acknowledge financial support from the National Natural Science Foundation of China (21673166), Wuhan Yellow Crane Talents of Science and Technology Plan, and the Fundamental Research Funds for the Central Universities (2015203020212).

References

- 1 I. Khairul, Q. Q. Wang, Y. H. Jiang, C. Wang and H. Naranmandura, Metabolism, toxicity and anticancer activities of arsenic compounds, *Oncotarget.*, 2017, **8**, 23905.
- 2 R. Stone, Arsenic and paddy rice: a neglected cancer risk?, *Science*, 2008, **321**, 184–185.
- 3 C. O. Abernathy, D. J. Thomas and R. L. Calderon, Health effects and risk assessment of arsenic, *J. Nutr.*, 2003, **133**, 1536S–1538S.
- 4 Z. Drobná, L. M. Del Razo, G. G. García-Vargas, L. C. Sánchez-Peña, A. Barrera-Hernández, M. Stýblo and D. Loomis, Environmental exposure to arsenic, AS3MT polymorphism and prevalence of diabetes in Mexico, *J. Exposure Sci. Environ. Epidemiol.*, 2013, **23**, 151–155.
- 5 S. Srivastava, Y. Chen and A. Barchowsky, Arsenic and cardiovascular disease, *Toxicol. Sci.*, 2009, **107**, 312–323.
- 6 M. F. Naujokas, B. Anderson, H. Ahsan, H. V. Aposhian, J. H. Graziano, C. Thompson and W. A. Suk, The broad scope of health effects from chronic arsenic exposure: update on a worldwide public health problem, *Environ. Health Perspect.*, 2013, **121**, 295.
- 7 J. J. Putila and N. L. Guo, Association of arsenic exposure with lung cancer incidence rates in the United States, *PLoS One*, 2011, **6**, e25886.
- 8 H. J. Sun, P. Xiang, J. Luo, H. Hong, H. Lin, H.-B. Li and L. Q. Ma, Mechanisms of arsenic disruption on gonadal, adrenal and thyroid endocrine systems in humans: A review, *Environ. Int.*, 2016, **95**, 61–68.
- 9 M. Valko, C. Rhodes, J. Moncol, M. Izakovic and M. Mazur, Free radicals, metals and antioxidants in oxidative stress-induced cancer, *Chem.-Biol. Interact.*, 2006, **160**, 1–40.
- 10 A. Kinoshita, H. Wanibuchi, M. Wei, T. Yunoki and S. Fukushima, Elevation of 8-hydroxydeoxyguanosine and cell proliferation via generation of oxidative stress by organic arsenicals contributes to their carcinogenicity in the rat liver and bladder, *Toxicol. Appl. Pharmacol.*, 2007, **221**, 295–305.
- 11 Y. Cheng, Y. Li, C. Ma, Y. Song, H. Xu, H. Yu, S. Xu, Q. Mu, H. Li and Y. Chen, Arsenic trioxide inhibits glioma cell growth through induction of telomerase displacement and telomere dysfunction, *Oncotarget.*, 2016, **7**, 12682.
- 12 W. Piao, D. Chau, L. Yue, Y. Kwong and E. Tse, Arsenic trioxide degrades NPM-ALK fusion protein and inhibits growth of ALK-positive anaplastic large cell lymphoma, *Leukemia*, 2017, **31**, 522–526.

- 13 Y. Liu, D. Duan, J. Yao, B. Zhang, S. Peng, H. Ma, Y. Song and J. Fang, Dithiaarsanes induce oxidative stress-mediated apoptosis in HL-60 cells by selectively targeting thioredoxin reductase, *J. Med. Chem.*, 2014, **57**, 5203–5211.
- 14 P. J. Dilda and P. J. Hogg, Arsenical-based cancer drugs, *Cancer Treat. Rev.*, 2007, **33**, 542–564.
- 15 X.-W. Zhang, X.-J. Yan, Z.-R. Zhou, F.-F. Yang, Z.-Y. Wu, H.-B. Sun, W.-X. Liang, A.-X. Song, V. Lallemand-Breitenbach and M. Jeanne, Arsenic trioxide controls the fate of the PML-RAR α oncoprotein by directly binding PML, *Science*, 2010, **328**, 240–243.
- 16 S. Gu, C. Chen, X. Jiang and Z. Zhang, ROS-mediated endoplasmic reticulum stress and mitochondrial dysfunction underlie apoptosis induced by resveratrol and arsenic trioxide in A549 cells, *Chem.-Biol. Interact.*, 2016, **245**, 100–109.
- 17 X.-Y. Fan, X.-Y. Chen, Y.-J. Liu, H.-M. Zhong, F.-L. Jiang and Y. Liu, Oxidative stress-mediated intrinsic apoptosis in human promyelocytic leukemia HL-60 cells induced by organic arsenicals, *Sci. Rep.*, 2016, **6**, 29865.
- 18 S. Shen, X.-F. Li, W. R. Cullen, M. Weinfeld and X. C. Le, Arsenic binding to proteins, *Chem. Rev.*, 2013, **113**, 7769–7792.
- 19 I. Pizarro, M. Gómez, C. Cámara and M. Palacios, Arsenic speciation in environmental and biological samples: extraction and stability studies, *Anal. Chim. Acta*, 2003, **495**, 85–98.
- 20 P. L. Toogood, Mitochondrial drugs, *Curr. Opin. Chem. Biol.*, 2008, **12**, 457–463.
- 21 J. S. Modica-Napolitano and K. K. Singh, Mitochondrial dysfunction in cancer, *Mitochondrion*, 2004, **4**, 755–762.
- 22 K. Jomova, Z. Jenisova, M. Feszterova, S. Baros, J. Liska, D. Hudecova, C. Rhodes and M. Valko, Arsenic: toxicity, oxidative stress and human disease, *J. Appl. Toxicol.*, 2011, **31**, 95–107.
- 23 S. Alarifi, D. Ali, S. Alkahtani, M. A. Siddiqui and B. A. Ali, Arsenic trioxide-mediated oxidative stress and genotoxicity in human hepatocellular carcinoma cells, *OncoTargets Ther.*, 2013, **6**, 75–84.
- 24 A.-S. Belzacq, C. El Hamel, H. Vieira, I. Cohen, D. Haouzi, D. Metivier, P. Marchetti, C. Brenner and G. Kroemer, Adenine nucleotide translocator mediates the mitochondrial membrane permeabilization induced by lonidamine, arsenite and CD437, *Oncogene*, 2001, **20**, 7579–7587.
- 25 M.-J. Hosseini, F. S. Shaki, M. Ghazi-Khansari and J. Pourahmad, Toxicity of arsenic(III) on isolated liver mitochondria: a new mechanistic approach, *Iran. J. Pharm. Res.*, 2013, **12**, 121–138.
- 26 D. Park, J. Chiu, G. G. Perrone, P. J. Dilda and P. J. Hogg, The tumour metabolism inhibitors GSAO and PENAO react with cysteines 57 and 257 of mitochondrial adenine nucleotide translocase, *Cancer Cell Int.*, 2012, **12**, 1.
- 27 C. Pace, T. D. Banerjee, B. Welch, R. Khalili, R. K. Dagda and J. Angermann, Monomethylarsonous acid, but not inorganic arsenic, is a mitochondria-specific toxicant in vascular smooth muscle cells, *Toxicol. in Vitro*, 2016, **35**, 188–201.
- 28 L. A. Pon and E. A. Schon, *Mitochondria*, Academic Press, 2011.
- 29 L.-Y. Yang, J.-L. Gao, T. Gao, P. Dong, L. Ma, F.-L. Jiang and Y. Liu, Toxicity of polyhydroxylated fullerene to mitochondria, *J. Hazard. Mater.*, 2016, **301**, 119–126.
- 30 F. Ricchelli, S. Gobbo, G. Moreno and C. Salet, Changes of the fluidity of mitochondrial membranes induced by the permeability transition, *Biochemistry*, 1999, **38**, 9295–9300.
- 31 P. Dong, J.-H. Li, S.-P. Xu, X.-J. Wu, X. Xiang, Q.-Q. Yang, J.-C. Jin, Y. Liu and F.-L. Jiang, Mitochondrial dysfunction induced by ultra-small silver nanoclusters with a distinct toxic mechanism, *J. Hazard. Mater.*, 2016, **308**, 139–148.
- 32 L. Biasutto, N. Sassi, A. Mattarei, E. Marotta, P. Cattelan, A. Toninello, S. Garbisa, M. Zoratti and C. Paradisi, Impact of mitochondriotropic quercetin derivatives on mitochondria, *Biochim. Biophys. Acta, Bioenerg.*, 2010, **1797**, 189–196.
- 33 J. Zhao, L. Ma, X. Xiang, Q.-L. Guo, F.-L. Jiang and Y. Liu, Microcalorimetric studies on the energy release of isolated rat mitochondria under different concentrations of gadolinium(III), *Chemosphere*, 2016, **153**, 414–418.
- 34 C.-F. Xia, J.-C. Jin, L. Yuan, J. Zhao, X.-Y. Chen, F.-L. Jiang, C.-Q. Qin, J. Dai and Y. Liu, Microcalorimetric studies of the effect of cerium (III) on isolated rice mitochondria fed by pyruvate, *Chemosphere*, 2013, **91**, 1577–1582.
- 35 J.-H. Li, X.-R. Liu, Y. Zhang, F.-F. Tian, G.-Y. Zhao, F.-L. Jiang and Y. Liu, Toxicity of nano zinc oxide to mitochondria, *Toxicol. Res.*, 2012, **1**, 137–144.
- 36 J. Zhao, Z.-Q. Zhou, J.-C. Jin, L. Yuan, H. He, F.-L. Jiang, X.-G. Yang, J. Dai and Y. Liu, Mitochondrial dysfunction induced by different concentrations of gadolinium ion, *Chemosphere*, 2014, **100**, 194–199.
- 37 J. Hu, V. K. Ramshesh, M. R. McGill, H. Jaeschke and J. J. Lemasters, Low Dose Acetaminophen Induces Reversible Mitochondrial Dysfunction Associated with Transient c-Jun N-Terminal Kinase Activation in Mouse Liver, *Toxicol. Sci.*, 2015, kfv319.
- 38 L. Yuan, T. Gao, H. He, F. L. Jiang and Y. Liu, Silver ion-induced mitochondrial dysfunction via a nonspecific pathway, *Toxicol. Res.*, 2017, **6**, 621–630.
- 39 S. Passarella, A. Atlante, D. Valenti and L. de Bari, The role of mitochondrial transport in energy metabolism, *Mitochondrion*, 2003, **2**, 319–343.
- 40 A. A. Gerencser, J. Doczi, B. Töröcsik, E. Bossy-Wetzel and V. Adam-Vizi, Mitochondrial swelling measurement in situ by optimized spatial filtering: astrocyte-neuron differences, *Biophys. J.*, 2008, **95**, 2583–2598.
- 41 K. Nowikovsky, R. J. Schweyen and P. Bernardi, Pathophysiology of mitochondrial volume homeostasis: potassium transport and permeability transition, *Biochim. Biophys. Acta, Bioenerg.*, 2009, **1787**, 345–350.
- 42 A. P. Halestrap and A. P. Richardson, The mitochondrial permeability transition: a current perspective on its identity and role in ischaemia/reperfusion injury, *J. Mol. Cell Cardiol.*, 2015, **78**, 129–141.
- 43 Z.-Y. Xu, M.-X. Zheng, Y. Zhang, X.-Z. Cui, S.-S. Yang, R.-L. Liu, S. Li, Q.-H. Lv, W.-L. Zhao and R. Bai, The effect

- of the mitochondrial permeability transition pore on apoptosis in *Eimeria tenella* host cells, *Poult. Sci.*, 2016, **95**, 198.
- 44 A. P. Halestrap, S. J. Clarke and I. Khaliulin, The role of mitochondria in protection of the heart by preconditioning, *Biochim. Biophys. Acta, Bioenerg.*, 2007, **1767**, 1007–1031.
- 45 M. Eskandari, V. Mashayekhi, M. Aslani and M. J. Hosseini, Toxicity of thallium on isolated rat liver mitochondria: the role of oxidative stress and MPT pore opening, *Environ. Toxicol.*, 2015, **30**, 232–241.
- 46 Y. Tsujimoto, T. Nakagawa and S. Shimizu, Mitochondrial membrane permeability transition and cell death, *Biochim. Biophys. Acta, Bioenerg.*, 2006, **1757**, 1297–1300.
- 47 M. K. Paul, R. Kumar and A. K. Mukhopadhyay, Dithiothreitol abrogates the effect of arsenic trioxide on normal rat liver mitochondria and human hepatocellular carcinoma cells, *Toxicol. Appl. Pharmacol.*, 2008, **226**, 140–152.
- 48 A. M. Spuches, H. G. Kruszyna, A. M. Rich and D. E. Wilcox, Thermodynamics of the As(III)-thiol interaction: arsenite and monomethylarsenite complexes with glutathione, dihydrolipoic acid, and other thiol ligands, *Inorg. Chem.*, 2005, **44**, 2964–2972.
- 49 A. P. Halestrap and C. Brenner, The adenine nucleotide translocase: a central component of the mitochondrial permeability transition pore and key player in cell death, *Curr. Med. Chem.*, 2003, **10**, 1507–1525.
- 50 F. Di Lisa, R. Menabo and A. Carpi, P429 The activity of monoamine oxidases is tightly related to mitochondrial membrane fluidity altered by aging, obesity and oxidative stress, *Cardiovasc. Res.*, 2014, **103**, S79–S79.
- 51 J. Garcia, R. Reiter, G. Ortiz, C. Oh, L. Tang, B. Yu and G. Escames, Melatonin enhances tamoxifen's ability to prevent the reduction in microsomal membrane fluidity induced by lipid peroxidation, *J. Membr. Biol.*, 1998, **162**, 59–65.
- 52 M. P. Murphy, How understanding the control of energy metabolism can help investigation of mitochondrial dysfunction, regulation and pharmacology, *Biochim. Biophys. Acta, Bioenerg.*, 2001, **1504**, 1–11.
- 53 C. Piccoli, R. Scrima, D. Boffoli and N. Capitanio, Control by cytochrome *c* oxidase of the cellular oxidative phosphorylation system depends on the mitochondrial energy state, *Biochem. J.*, 2006, **396**, 573–583.
- 54 L. Kussmaul and J. Hirst, The mechanism of superoxide production by NADH: ubiquinone oxidoreductase (complex I) from bovine heart mitochondria, *Proc. Natl. Acad. Sci. U. S. A.*, 2006, **103**, 7607–7612.
- 55 P. M. Keeney, J. Xie, R. A. Capaldi and J. P. Bennett, Parkinson's disease brain mitochondrial complex I has oxidatively damaged subunits and is functionally impaired and misassembled, *J. Neurosci. Res.*, 2006, **26**, 5256–5264.
- 56 G. Petrosillo, M. Matera, N. Moro, F. M. Ruggiero and G. Paradies, Mitochondrial complex I dysfunction in rat heart with aging: critical role of reactive oxygen species and cardiolipin, *Free Radical Biol. Med.*, 2009, **46**, 88–94.
- 57 X. Shen, M. Jin, C. Zhao, X. Tan, H. Liu, X. Qin, Z. Qiu and Y. Liu, Microcalorimetric study of the effect of artesunate on the growth metabolism of mitochondria isolated from rat liver, *J. Therm. Anal. Calorim.*, 2013, **111**, 1947–1952.